Chapter

Sea Almond as a Promising Feedstock for Green Diesel: Statistical Optimization and Power Rate Law Based Chemical Kinetics of Its Consecutive Irreversible Methanolysis

Chizoo Esonye, Okechukwu Donminic Onukwuli, Akuzuo Uwaoma Ofoefule, Cyril Sunday Ume and Nkiruka Jacintha Ogbodo

Abstract

For successful industrial scale-up and effective cost analysis of transesterification process, presentation of complimentary research data from process optimization using statistical design techniques, chemical kinetics and thermodynamics are essential. Full factorial central composite design (FFCCD) was applied for the statistical optimization of base methanolysis of sea almond (*Terminalia catappa)* seed oil using response surface methodology (RSM) coupled with desirability function analysis on quadratic model. Reaction time had the most significant impact on the biodiesel yield. Optimum conditions for biodiesel yield of 93.09 wt% validated at 92.58 wt% were 50.03°C, 2.04 wt% catalyst concentration, 58.5 min and 4.66 methanol/oil molar ratio with overall desirability of 1.00. Ascertained fuel properties of the FAME were in compliance with international limits. GC–MS, FTIR and NMR characterizations confirmed unsaturation and good cold-flow qualities of the biodiesel. Based on power rate law, second-order kinetic model out-performed first-order kinetic model. Rate constants of the triglyceride (TG), diglycerides (DG) and monoglycerides (MG) hydrolysis were in the range of 0.00838–0.0409 wt%/min while activation energies were 12.76, 15.83 and 22.43 kcal/mol respectively. TG hydrolysis to DG was the rate determining step. The optimal conditions have minimal error and would serve as a springboard for industrial scale-up of biodiesel production from *T. catappa* seed oil.

Keywords: kinetics, methanolysis, optimization, response surface methodology, sea almond

1. Introduction

The application of biodiesel as an alternative energy source to petrodiesel due to its various established renewable advantages has been reported by many researches [1].

Most importantly the biodiesel production from low cost feedstocks (mostly from agro-waste) that are readily and widely available, with high oil yield, non-food competing and underutilized are key parameters that make them satisfactory to EU sustainable biofuel directives. Various methods have been established as ways of converting vegetable oils into petrodiesel-replaceable-form for application in diesel engines (DE). It is very important to highlight that pyrolysis as thermal degradation of vegetable oil produces more bio-gasoline than biodiesel fuel, micro-emulsion results have been only on short term while dilution of vegetable oil with petrodiesel requires very low concentration of vegetable oil. Transesterification is therefore the major chemical process that involves the conversion of fatty acids or triglycerides in vegetable oils to biodiesel (alkyl esters). Structures of chemical building blocks (CBB) involved in transesterification process are presented in **Figure 1**. Although transesterification of vegetable oils can be conducted with both homogeneous (acid or base) and heterogeneous catalysts, base methanolysis always provide much faster rates [2] and cheaper process [1] and more predominantly applied for industrial purposes and large scale biodiesel production. However, currently the major challenge of biodiesel application as a replacement to petrodiesel is its industrial production sustainability. This can be achieved through detailed established transesterification viability and most importantly feasibility data.

Consequently, the successful scale-up of laboratory results in transesterification requires so much information obtained through optimization and kinetics studies. Hence, for effective cost analysis of transesterification process, a holistic presentation of research data from process optimization using statistical design techniques and knowledge of chemical kinetics are essential in establishing the optimum conditions, feed compositions, degree of conversion and recycling as well as reaction mechanisms. It has been established that one factor at a time (O-F-AT) has obvious challenges of non-reliability of obtained results, non-depiction of the interactive effects of the independent variables and ineffectiveness due to the existence of multiple experimental run [3]. Therefore, many researches on optimization and modeling of transesterification process have been established through the application of such soft computing techniques like response surface methodology (RSM), artificial neural network (ANN) and integrated models (IM) [4]. It is very interesting to write that RSM has undisputable edge over others due to its ability to navigate the design space, flexibility, robustness in establishing the optimum condition with the help of desirability function and capability to minimize the number of experimental runs needed to give adequate evidence for statistically acceptable result [4]. Other obvious advantages are its availability in most statistical software, as an asset in statistical quality control, expression and inferential statistics, reliability, gage repeatability and reproducibility studies and process ability as well as improved grappling output. The integration of RSM with desirability function has been reported to have a high a potential over conventional RSM [5]. In the RSM design of experiment, different types have been applied such as full factorial, fractional factorial, Box-Behken, Placket-Burman, central composite rotatable design (CCRD) etc. However, full factorial central composite design (FFCCD) has the advantage of providing double factor axial points at a fixed distance from the centre and significant replicate points at the centre. This has a resultant effect of providing a better reduced-cost approach in obtaining optimal response with least number of experimental runs.

Also, it has been reported that lack of the vital kinetics data of many non-conventional biodiesel feedstocks possess great challenges on their industrial scale process application, reactor design, simulation and control [1]. Although, many researchers have previously reported the kinetics of base-catalyzed transesterification of conventional feedstocks, those works have dwelled more on the reversible

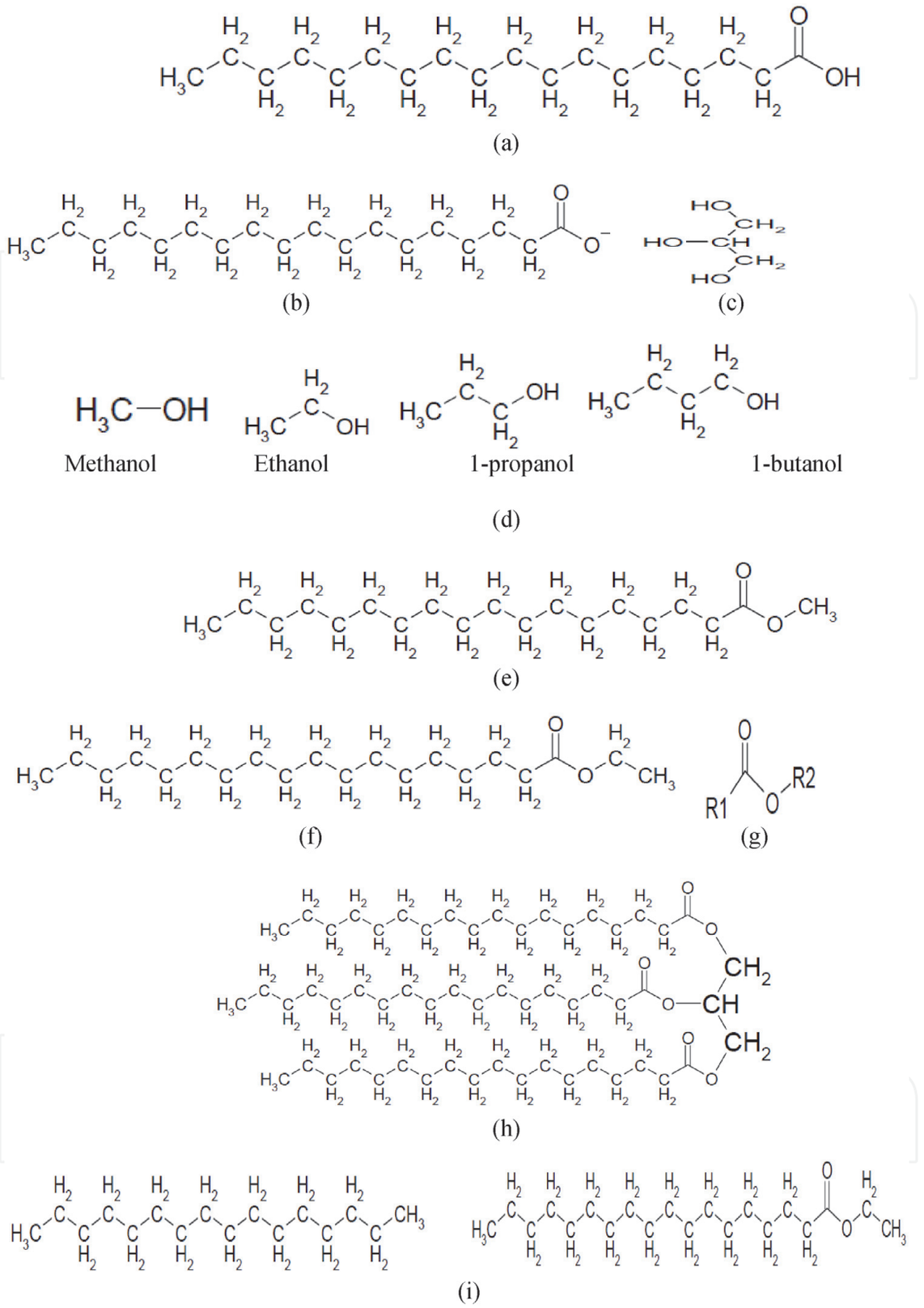

Figure 1.
Structures of chemical building blocks involved in transesterification process. (a) Idealized fatty acid; (b) idealized soap; (c) glycerol; (d) alcohols used in biodiesel production; (e) methyl ester; (f) ethyl ester; (g) generalized ester structure; (h) Trigyceride. (i) Cetane versus ethyl ester.

consecutive mechanisms using complex kinetic models. Such works on sunflower oil ethanolysis [6], jatropha oil methanolysis (Kuma et al., 2011), African pear seed oil [1], mixed crude oil palm oil methanolysis [7] buttress the above point. It is noteworthy that the complexity in kinetic models proposed in the above reports challenges their industrial translation while simplified kinetic models suffice for practical

purposes. Consequently, methanolysis reaction has been proposed to constitute three consecutive irreversible stages, more especially by the usual condition of using high methanol to oil ratio (>3:1) which shifts the reaction methyl to the right [8, 9].

Terminalia catappa; belongs to *combietaccea* family with meridional Asian origin. It occurs in nature and widespread in the sub-tropical zones of India. It is called sea almond or tropical almond or Indian almond. In Nigeria, it is grown basically for

Figure 2.
Sea almond fruit biomass, a. the fruit, b. fruit cut section, c. dried fruit pulp, d. inner seed with coat. e. the seed, f. the fruit husk, g. the ground pulp (raffinnate and 600 μm particle size).

ornamental purposes [10]. It has been reported that the major works on *Terminalia catappa*, has focused mainly on the investigations of phyto-chemical, biological and medicinal application of its leaves, bark and fruit extracts with little or no attention to its seed oil industrial application [11]. Similar to other almonds like Iranian bitter almond and sweet almond, sea almond contains high amount of oil (>60%) [4, 12]. This is similar in quantity to what is observed in other established viable biodiesel feedstocks such as sunflower, peanut and rape seed [11]. Although empirical non-linear kinetics model of oil extraction as well as synthesis of transformer oil from seeds of *T. catappa* has been reported [11], process optimization and the kinetics of its seed oil methanolysis based on irreversible model under consecutive mechanism has not been reported. A pictorial representation of the *T. catappa* is shown in **Figure 2**. It is therefore the aim of this study to investigate and establish the optimal conditions, chemical kinetics and thermodynamic data for the production of biodiesel from *T. catappa* (sea almond) for its biofuel application relevance. This research is believed to compliment *T. catappa* seed oil's bio-lubricant potential as previously reported [11]. Additionally, the relevant characterizations through the application of nuclear magnetic resonance, gas chromatographic - mass spectrometry, Fourier transform infrared spectrometry analysis of the biodiesel were conducted and reported.

2. Materials and methods

2.1 Reagents

All the reagents used were all of analytical grade and purchased from the popular BriDGe-Head Chemical market in Onitsha, Anambra State Nigeria.

2.2 Biomass collection and preparation

2.2.1 Sourcing of seeds/seed meal preparation

The ripped fruits were collected from Abakaliki city of Nigeria. They were subsequently washed to remove dirt before the pulp was peeled out to release the kernel. The kernels were placed on solar drier for one (1) week. The seeds were extracted by cracking the kernels. Electric milling machine was used to grind the seeds into micro-sized meals before being sieved using an electric powered mechanical sieve to obtain a fine size of the meal. The remaining moisture in the sieved ground meal was removed by further sun drying the meal for a period of 5 days.

2.3 Oil extraction and degumming

The oil extraction followed the same method previously applied by the authors [1] but with slight modification. The extracted oil was further degummed by mixing the raw oil with 3 wt% by weight of warm water and the mixture was mechanically agitator coupled with using magnetic stirrer for 30 minutes at a temperature of 60° C to ensure that the emulsifiers were easily separated from the oil [13].

2.4 Physico-chemical characterization of the oil

The quality of the seed oil was determined in accordance with Association of Official Analytical Chemist [14] method. Other properties such as moisture, viscosity and density content were ascertained by using oven method, Oswald viscometer

apparatus and density bottle respectively. The ash content and the refractive index were also measured with Veisfar muffle furnace and Abbe refractometer respectively. All the analyses were repeated three times and the average values were calculated and reported.

2.5 Base methanolysis process

The process follows the approach previously applied in Ofoefule et al. [13] with slight deviations. The extracted and pre-treated oil (100 ml) was first preheated to 80°C for 30 min before adding sodium methoxide. Sodium methoxide is more effective than direct mixing of sodium hydroxide due to the fact that direct mixing of NaOH with methanol produces water through hydrolysis and this affects the biodiesel yield. Therefore, sodium methoxide was prepared using the method previously reported by the authors [1]. Then the seed oil mixed with sodium methoxide at methanol/oil molar ratio of 6:1 was kept at 65°C for 65 min. This process was conducted in a 500 ml reflux condenser fitted with heater and stirrer. The process was conducted at atmospheric pressure and 140 rpm.

The biodiesel mixed with glycerine was separated, washed and dried according to the method previously applied by the authors [1]. The percentage biodiesel yield was calculated by using Eq. (1)

$$FAME\ yield(\%) = \frac{W_{FAME}}{W_{seed\ oil}} x100 \tag{1}$$

where $W_{FAME=weight\ of\ fatty\ acid\ methyl\ ester\ after\ methanolysis}$

$$W_{seedoil=weight\ of\ seed\ oil\ used\ for\ the\ base\ methanolysis.}$$

2.5.1 Physico chemical characterization of the biodiesel

The necessary fuel related physico-chemical properties of the biodiesel produced were determined using ASTM and AOAC [14] standard methods. ASTM D standards were used to determine the kinematic viscosity, density, pour, cloud, flash points, acid value and calorific values while AOAC methods were used to determine specific gravity, Iodine value and refractive index. ASTM D-445 method, the density was determined by ASTM D − 1298 method. The pour, flash and cloud points determinations were done using ASTM D-97, ASTM D-93, ASTMD-2500b methods respectively while acid value was measured by ASTM D-664 method. The refractive index was determined using AOAC 921.08. The specific gravity was ascertained using AOAC 920.212 and iodine value using AOAC 920:159 while moisture content was obtained using air-oven method. The cetane index (CI), cetane number (CN) and higher heating values were ascertained using standard correlations previously applied in [13].

2.5.2 Chemical characterization of seed oil and biodiesel

2.5.2.1 Nuclear magnetic resonance (NMR) analysis

The ^{13}C NMR of the sample was recorded on a Bruker Am-400 spectrometer operating at 100.6 MHz. The gated decoupling pulse sequence was used with the following parameters: Number of seans 512, acquisition time 1.366 s pulse with 10.3 s delay time 1.0 s. FID (free induction decay) was transformed and zero filled

to 300 k to give a digital resolution of 0.366 Hz/point. Proton nuclear magnetic resonance (^{1}H NMR) spectra were recorded by dissolving approximately 100 mg sample 1 ml of deuterated chloroform solution and analysis using a Brucker model AC-250 spectrometer. Chemical shifts were measured in ppm downfield from internal tetramethyl siltane. The following instrumental parameters were applied. Spectrum width – 5000 Hz; acquisition time – 3.2775; delay time – 1 s and pulse width – 7 μsec.

2.5.2.2 Fourier transform infrared spectroscopic analysis of the oil and biodiesel

FT-IR analysis was performed to monitor the functional groups in the seed oil. The mid infrared spectra of oil samples were obtained in Fourier transform spectrometer by IR Affinity-1 Shimadzu, model No: 3116465. The FT-IR has SN ratio of its class of 30,000:1, 1 minute accumulator in the neighborhood of 2100 cm^{-1} peak to peak with a maximum resolution of 0.5 cm^{-1} in the region of 400 cm^{-1}-4000 cm^{-1}. It has microlab software as supporting software. The method of sample introduction was through sample cell. Cleaning of the cell was done with trisolvent mixture of acetone-toluene-methanol before background collection. About 0.5 ml of the sample (oil) was taken using the sample cell and introduced into the cell unit of the system. The scan results were obtained on the incorporated computer system as spectra. The peaks of the spectra obtained were identified and interpreted to identify the functional groups in the molecules of the oil with the aid of structure correlation chart [15].

2.5.2.3 Gas chromatographic-mass spectroscopic (GC: MS) analysis of the fatty acid profile of the biodiesel

The process followed the method reported by Esonye et al. [4]. The fatty acid composition of the biodiesel samples was in accordance with AOAC official method Ce2–66 using GCMS-QP2010 plus, Shimadzu. GC–MS is faster than the conventional GC; it equally provides molecular weight information and requires an aliquot sample. The GC–MS fragments the analyte to be identified on the basis of its mass and the column was calibrated by introducing methyl ester standards while good separations were achieved by diluting the sample in a little quantity of ethyl acetate. In this study, hydrogen served as the carrier gas and its flowrate was controlled at 41.27 ml/min while the flowrate of the column was 1.82 ml/min. Oven temperature was fixed at 80°C prior ramping up at 6°C/min and then up till 340°C. The Peaks identification was carried out by comparing their retention time and mass spectra with Mass Spectra Library (MSL) [16].

2.6 Optimization using RSM-desirability function techniques

2.6.1 Design of Experimental and Statistical Analysis

Central composite design (CCD) was applied in developing the design of experimental (DOE) for the base methanolysis of the *Terminalia catappa* seed oil. The matrix of the DOE based on the full factorial pattern provided sixteen (16) factorial points, eight (8) axial points and six (6) center points and these clearly present the required information on the inner conditions of the experimental circle. Design expert 7.0.0 software was employed for the design of the four (4) independent variables (n = 4), each with two (2) different levels. The total number of experiments (N) was worked out as $N = (n^2 + 2n + n_c) = 16 + 2(4) + 6 = 30$. This includes the standard 2n factorial points with their origin at the centre, 2n axial points fixed

at a distance α from the centre to generate the quadratic terms and n_c replicate points at the centre. After defining the range of each of the process variable, they were coded to lie at ±1 for the fractional points, 0 for the centre point, ±α for the axial points. The numerical values of the variables were transferred into their respective coded values as shown in Eq. (2). The factor levels were coded as -α to +α as shown in the **Table 1** based on fuel factorial composite design (FFCDD). X_{min} (−α) and X_{max} (+α) are minimum and maximum values of X respectively, −1 and + 1 have a level of variance of $(X_{min} + X_{max})/2$ $(X_{max} - X_{min})/2b$ and 0 has a level of variance of $(X_{min} + X_{max})/2$. The effects of selected factors on the biodiesel yield were investigated based on the experimental conditions of the thirty set that were conducted. The main operating conditions (reaction time, alcohol to oil molar ratio, catalyst weight and reaction temperature) that conventionally affect methanolysis for biodiesel production were studied. **Table 1** contains the levels and range of the four independent variables. The variables range was chosen based on results obtained from previous works [17]. The presence of a clear curvature for the methanolysis resulted in selecting a second-order (Eq. (3)) for the transesterification [13].

$$X_i = \frac{2X - (X_{max} - X_{min})}{X_{max} - X_{min}} \tag{2}$$

$$Y = \beta_0 + \sum_{i=1}^{n} \beta_i x_i + \sum_{i=1}^{n} \beta_{ii} x_i^2 + \sum \sum_{i=1}^{n} \beta_{ij} x_{ij} \tag{3}$$

where, *Xi* - required coded value of a variable, X_{min} and X_{max} - the low and high values of *X* respectively, Where β_0 - a constant, β_i - the linear coefficient, β_{ii} – the quadratic coefficient, β_{ij}-interactive coefficients, X_i and X_{ij} are the uncoded independent variables and *Y*- predicted response (%). The fitted quadratic model equations obtained from regression analysis were used for the successful development of the response surface plots. The desirability function method was employed in order establish an efficient approach for achieving maximum FAME production. The application of one side transformation (Eq. (4)) followed by overall desirability (*D*) (Eq. (5)) using univariate technique was adopted [5, 13].

$$d_i = \begin{cases} 0 \; Y_i \le Y_{i-min} \\ \left[\dfrac{Y_i - Y_{i-min}}{Y_{i-max} - Y_{i-min}}\right] Y_{i-min} < Y_i < Y_{i-max} \\ 0 \; Y_i \ge Y_{i-max} \end{cases} \tag{4}$$

$$D = \left(d_1^{w1} d_2^{w2} d_3^{w3} d_4^{w4} d_5^{wn}\right)^{1/\sum wi} \tag{5}$$

Parameters/Units	Symbols	Coded levels				
		-α	-1	0	1	+α
Temperature (°C)	X_1	30	40	50	60	70
Catalyst conc. (%wt)	X_2	0.5	1.0	1.5	2.0	2.5
Reaction time (min.)	X_3	45	50	55	60	65
Alcohol/Oil molar ratio	X_4	3:1	4:1	5:1	6:1	7:1

Table 1.
Variables, their symbols and CCD coded levels for Terminalia catappa *seed oil methanolysis.*

Where d_i is individual response desirability, Y_i is the response values, $Y_{i\text{-}min}$ is the minimum acceptable value for response i and $Y_{i\text{-}max}$ is the maximum acceptable value for response i. D is the overall desirability, wi is a weighed composite desirability.

The statistical methods used to ascertain the degree at which the models represent the experimental data were done by determining the coefficient of determination, (R^2) adjusted coefficient of determination (Adj. R^2), the mean squared error (MSE), root mean squared error (RMSE), the standard error prediction (SEP) and average absolute deviation (AAD) [13].

2.7 Chemical kinetic study

The rate of reaction and its mechanism as regards to the methanolysis process of the seed oil were investigated by considering irreversible conditions.

2.7.1 Equation of methanolysis reaction

It has been reported that the conventional transesterification mechanism could be represented by three consecutive irreversible [8] reactions as represented in Eqs. (6)–(8) with Eq. (9) being the summary of the Equations.

$$TG + AOH \underset{\rightarrow}{k_1} DG + BD \tag{6}$$

$$DG + AOH \underset{\rightarrow}{k_2} MG + BD \tag{7}$$

$$MG + AOH \underset{\rightarrow}{k_3} Gl + BD \tag{8}$$

$$\begin{array}{cccccc} CH_2OCOR & & & CH_2OH & & R'COOR \\ CHOCOR & + & 3ROH & \leftrightarrow & CHOH & + & R"COOR \\ CH_2OCOR & & & & CH_2OH & & R"'COOR \\ \text{Triglycerides} & & \text{Alcohol} & & \text{Glycerol} & & \text{Biodiesel} \end{array} \tag{9}$$

Where MG is monoglycerides, DG is Diglyceride, TG is Triglyceride, Gl is Glycerol, AOH is alcohol and BD is Biodiesel.

2.7.2 Irreversible model assumptions

Since simplified kinetic models suffice for practical purposes, experimental data were processed under the following assumptions [2, 8, 9]:

1. The methanolysis reaction is constituted by three consecutive stages but assumed irreversible because of the excessive presence of methanol in the reaction [9].

2. The free fatty acid neutralization was insignificant since the free fatty acid was negligible.

3. The saponification reaction was considered insignificant because of low acid value of the oil.

2.7.3 The kinetic experimental conditions

Kinetics experimental design (KED) of the methanolysis process of the sea almond seed oil followed the method previously reported by the authors in

Esonye et al. [1] with slight deviations to ascertain the kinetics and thermodynamic requirements. To examine the temperature dependency of the reaction rate constants, three (3) level temperatures (55–65°C) and twelve (12) intervals of reaction time (0-100 min) were considered at 6:1 alcohol (methanol)/sea almond seed oil molar ratio. About 2 ml aliquot sample were withdrawn at specified time intervals from the reactor, introduced into a test tube in an ice bath to quench the reaction. The content of the composite sample was obtained using a gas chromatography [1]. The G.C was equipped with split/splitless injection system operating at 185 degree Celsius, split ratio of 100:1, sample volume of 0.3 μL. High purity hydrogen gas was used as drag.

2.7.4 Second: order irreversible kinetic model

The best kinetic model for an irreversible model has been proposed to be a second-order based on TG hydrolysis especially during the early stages of the reaction [8]. To test the above report, a model developed based on TG hydrolysis and the second-order reaction rate for TG would be as shown in Eq. (10) [18].

$$\frac{-\mathrm{d}[\mathrm{TG}]}{\mathrm{dt}} = \mathrm{k}[\mathrm{TG}]^2 \tag{10}$$

Resolving Eq. (10) further yields Eq. (11).

$$k_{TG}t = \frac{1}{[\mathrm{TG}]} - \frac{1}{[\mathrm{TG0}]} \tag{11}$$

Where k is the overall rate constant, t is the reaction time, TG_0 is the initial triglyceride concentration.

A plot of reaction time (t) against $\frac{1}{[\mathrm{TG}]}$ will give a straight line if the model is valid. Where k is the overall rate constant, t is the reaction time; TG_0 is the initial triglyceride concentration. A plot of reaction time (t) against $\frac{1}{[\mathrm{TG}]}$ will give a straight line if the model is valid. Similar approach was applied on the monoglycerides and diglycerides hydrolysis to get Eqs. (12) and (13).

$$k_{DG}t = \frac{1}{[DG]} - \frac{1}{[DG_0]} \tag{12}$$

$$k_{MG}t = \frac{1}{[MG]} - \frac{1}{[MG_0]} \tag{13}$$

2.7.5 First-order irreversible kinetic model

To determine the kinetics of the reaction based, the effect of reaction temperature and time were measured. It was assumed that the catalyst was used in sufficient amount with respect to oil to shift the reaction equilibrium towards the formation of fatty acid methyl esters. Thus, the reverse reaction could be ignored and change in concentration of the catalyst during the course of reaction can be assumed to be negligible [19]. Also, since the concentrations of both DG and MG were found to be very low (DG < 2.9 wt%, MG < 1.45 wt%) compared to those of TG (TG > 94 wt%) in the crude vegetable oils used in this research, the reaction could be assumed to be a single-step transesterification [20]. Therefore, the rate law of the transesterification reaction for forward reaction can be expressed by Eq. (14).

$$-r_{TG} = \frac{-d[TG]}{dt} = k'.[TG].[ROH]^3 \tag{14}$$

Where [TG] is the concentration of triglycerides and [ROH] that of methanol and k′ is the equilibrium rate constant. This overall reaction follows a second-order reaction rate law. However, due to the high molar ratio of methanol to oil, the change in methanol concentration can be considered as constant during reaction. This means that by taking methanol in excess, its concentration does not change the reaction order and it behaves as a first-order chemical reaction. Hence, the reaction would obey pseudo-first order kinetics [19] and finally, the rate expression can be written as in Eq. (15).

$$-r_{TG} = \frac{-d[TG]}{dt} = k.[TG] \tag{15}$$

Where k is modified rate constant and $k = k'[ROH]^3$. Assuming that the initial triglyceride concentration was $[TG_0]$ at time t = 0, and at time t it falls down $[TG_t]$. The integration of Eq. (15) for t = 0, $[TG] = [TG_0]$ and at t = t, $[TG] = [TG_t]$ gives Eq. (16):

$$-\ln[TG] + \ln[TG_0] = kt \tag{16}$$

In order to test the rate equation in Eq. (16), the experimental data were fitted to a straight line while the coefficient of determination was ascertained. A plot of –ln [TG] against time was obtained.

2.7.6 Thermodynamic requirement

In order to ascertain the process thermodynamic requirement, the values of rate constants were used to determine the Arrhenius activation energy from the plots of reaction rate constant (k) versus the reciprocal of absolute temperature (T) (Eq. (17)). DG and MG relationship with time followed the same trend with that of TG.

$$\log k = k_0 - \frac{E_a}{2.303R}\left(\frac{1}{T}\right) \tag{17}$$

Where E_a = Activation energy, R = Gas constant (8.314×10^{-3} J/Kmol), K = rate constant, K_O = frequency factor.

3. Results and discussion

3.1 Physico-chemical characterization result

The fuel related properties of the biodiesel and its parent oil obtained from this work at the optimum conditions are presented in **Table 2**. The properties of the biodiesel compared well with the American standards, European specification and other feedstocks recently applied for biodiesel production [4, 21]. The viscosity of the sea almond compared well with standards and other similar varieties. This is very important for the efficiency of its engine application since many diesel engines used injection pumps that do not accept high viscous fluids that clog the fuel filteration units. Also, sea almond had a better cetane number than Iranian bitter

Parameters	Sea almond seed oil[1]	Sea almond seed oil FAME[1]	Sweet almond seed oil FAME[2]	Iranian bitter almond seed oil FAME[3]	Standards		
					ASTM D 9751	ASTMD 6751	EN 14214
Oil/Biodiesel yield (%)	60.57	94.21	94.90	—	—	—	—
Density (kg/m^3)	856.10	855.3	849.1	887	850	880	860–900
Moisture content (%)	0.66	0.02	0.02	—	—	—	—
Refractive index	1.4471	1.441	1.4402	—	—	—	—
Acid value (mgKOH/g)	2.701	0.37	0.46	0.44	0.062	0.50	0.50
Free fatty acid (%)	1.35	0.18	0.23	—	0.31	0.25	0.25
Iodine value (mgKOH/g)	38.11	27.11	28.02	117.29	42–46	—	120max.
Saponification value (mgKOH/g)	166.21	162.3	161.05	185.35	—	—	—
Ash content (%)	1.00	0.01	0.01	—	0.01	0.02	0.02
Kinematic viscosity (mm^2/s)	—	2.40	2.52	4.68	2.6	1–9-6.0	3.5–5.0
Smoke point (°C)	40	36	34	—	—	—	—
Fire point (°C)	—	40	40	—	—	—	—
Flash point (°C)	156	138	136	173	60–80	100–170	120
Cloud point (°C)	−3	-3	−2	10	−20	−3 to 12	—
Pour point (°C)	—	−7	−6	−3	−35	−15 to 16	—
Calorific value (KJ/Kg)	—	32,188.50	31,178.39	—	42–46	—	35
Conductivity (Us/CM)	—	0.45	0.40	—	—	—	—
Cetane index	—	72.0	73.0	—	—	—	—
Cetane number	—	70.60	70.40	44.6	40–55	47 min.	51 min.
Higher heating value (HHV)[a] (MJ/kg)	—	35.62	34.72	—	—	—	—
Higher heating value (HHV)[b] (MJ/kg)	—	41.66	40.76	—	—	—	—
Higher heating value (HHV)[c] (MJ/kg)	—	64.65	63.75	—	—	—	—

[a]*Based on flash point.*
[b]*Based on viscosity.*
[c]*Based on density, min-minimum, max- maximum.*
[1]*This study.*
[2]*[4].*
[3]*[21]*

Table 2.
Physico-chemical properties of the sea almond seed oil and its FAME, sweet almond biodiesel and Iranian bitter almond biodiesel versus standards.

almond but compared well with sweet almond variety and standard specifications. This shows that sea almond oil is less unsaturated than Iranian bitter almond sea oil which has been reported to have 84.7% unsaturation [21] against 55.32% from sea almond and 52.42% for sea almond. The iodine value of sea almond was observed to be five (5) times less than Iranian bitter almond. Although Iranian bitter almond biodiesel iodine value is similar to that of tiger nut oil, the low value of sea almond

biodiesel iodine value indicates less unsaturation. It equally shows that sea almond biodiesel will be comparatively less prone to oxidation instability and glyceride polymerization that normally leads to formation of deposits. The flash point, cloud point and pour point of Iranian bitter almond were very high compared to standards and the values recorded for both sea and sweet almond varieties. It implies that Iranian bitter almond variety will be safer to transport and handle in terms of flammability status and as well as be less suitable for winter season operations when compared with the hazardous and cold flow properties of sea almond. The parent oil characteristics of sea almond exhibited improved properties as a result of the base methanolysis [1].

3.2 FTIR characterization result

Table 3 contains peaks identified from the spectrum of the sea almond seed oil and its biodiesel. The band regions between 1734.60 cm^{-1}-1860.18 cm^{-1} and 1734.60 cm^{-1} - 1819.44 cm^{-1} for the oil and its biodiesel respectively can be ascribed to the stretching vibrations of C=O group. It shows the conversion of the triglyceride in the parent oil to biodiesel (methyl esters). Also, the specific bands of 2421.18 cm^{-1} and 2411.21 cm^{-1} appear with alkenes group for triglyceride and its biodiesel respectively. Also, the band regions between 3373.44–3495.22 cm^{-1} and 3365.18–3598.44 cm^{-1} for the parent seed oil and its biodiesel respectively can be ascribed to single-bonded hydroxyl group (O–H) stretching vibrations, appearing at high energy positions [4]. The single bond functional group O-H was observed to be prevalent in the biodiesel with stretch vibrations [4]. The presence of water molecule was evidenced by the hydrogen bonding [22]. The presence of C-H at 1357.64, 1474.28 and 1522.72 cm^{-1} regions of the biodiesel spectrum can be attributed to the properties such as pour and cloud points that influence the performance of biodiesel during cold weather engine operation [22]. However, the presence of carbon to

Sea almond seed oil			Sea almond seed oil biodiesel		
Wave number (cm^{-1})	**Type of Vibration**	**Functional group**	**Wave number (cm^{-1})**	**Type of vibration**	**Functional group**
892.50	Bending	=C-H	892.50	Bending	=C-H (alkenes)
1076.70	Bending	C-O-C	1041.96	Stretching	C-O
1188.64	Stretching	C-O	1134.60	Split rocking	C-O
1317.66	Bending/rocking	CH_2	1197.20	Split rocking	C-O
1474.28	Bending/rocking	CH_2	1317.66	Bending/Rocking	CH_2
1500.50	Bending/rocking	CH_2	1474.28	Bending/Rocking	CH_2
1734.60	Stretching	C=O	1555.12	Bending/Rocking	CH_2
1860.18	Stretching	C=O	1734.60	Stretching	C=O
2421.18	Symmetrical/ Stretching	C=C	1819.44	Stretching	C=O
3373.44	Stretching	O-H	2411.21	Symmetrical/ Stretching	C=C
3495.74	Stretching	O-H	3365.18	Stretching	O-H
			3598.44	Stretching	O-H

Table 3.
FT-IR main characteristic band positions for se almond seed oil and its biodiesel.

carbon (C=C) unsaturated bonds can cause the biodiesel samples to remain in liquid state but may be liable to poor storage stability due to oxidation. This implies that the biodiesel would not need cold flow improver for better performance. All the absorptions corresponding to C-O and C=O stretches indicate that the biodiesel product contains ester functional groups typical to any biodiesel type, while the following groups: C–H, C=H, and O–H indicated biodegradability of the oil and produced biodiesel [11]. Significant differences were effected by the ester groups. The specific peak that appeared at 892.50 cm^{-1} possesses bending type of vibrations appearing at low energy and frequency region in the spectra. It indicates the presence of = C–H functional groups [4]. It is part of fatty acid methyl ester with unsaturated bond in the seed oil and ester [23]. The specific peaks found in the region of 1088.80 cm^{-1} and 1197.20 cm^{-1} show split stretching and rocking vibrations of the carbonyl group (C–O) for the triglyceride and its methyl ester respectively [24]. The bending and rocking vibrations of methyl group in the parent oil and its methyl ester appeared between 1317.66–1500.50 cm^{-1} and 1317.66–1555.12 cm^{-1} respectively [25].

3.3 GC-MS characterization result

The various fatty acids present in the sea almond biodiesel are presented in **Table 4** in an increasing order of their retention time. A total of 38.14% saturated fatty acid, 39.92% monounsaturated fatty acid and 12.50% polyunsaturated fatty acids were found to be contained in the biodiesel The presence of high level of

Peak No.	Retention time (min.)	Fatty acid methyl ester	Amount (%)
1.	3.874	Capric acid	1.06
2.	4.017	Caprylic acid	1.14
3.	4.357	Stearic acid	1.24
4.	4.866	Eicosenic acid	8.14
5.	5.289	Erucic acid	0.75
6.	5.788	Palmitic acid	8.23
7.	6.729	Lignoceric acid	3.75
8.	7.243	Oleic acid	39.34
9.	8.922	α- Linolenic acid	9.07
10.	11.044	Palmtoleic acid	0.66
11.	11.281	Elaidic acid	1.09
12.	12.999	Arachidic acid	3.30
13.	14.569	Behenic acid	3.66
14.	16.888	Myristic acid	3.88
15.	18.367	Margaroleic acid	1.18
16.	22.223	Linoleic acid	0.72
17.	22.781	Gadoliec acid	0.12
18.	23.770	Lauric acid	1.66
19.	23.995	γ-linolenic acid	3.21
20.	23.875	Vaccenic acid	2.01

Table 4.
Fatty acid profile of the sea almond seed oil biodiesel.

monounsaturated fatty acids in methyl esters translates to high biodiesel quality [26]. Therefore, the high levels of monounsaturated fatty acids (39.92%) contained in the sea almond seed oil methyl ester is expected to make it possess excellent fuel qualities. Also, the higher the amount of unsaturated fatty acid in a biodiesel sample, the better the cloud point but lower the oxidation stability which implies that the higher composition of unsaturated fatty acids in the methyl ester (52.42%) would therefore enhance its cold flow properties [27]. It is reported that the high viscous nature of waste frying oils is because of their high saturated and less unsaturated fatty acids and this could cause micro-crystal formations that are dangerous to engine fuel injection units [28, 29]. Therefore, the application of biodiesel derived from the kernel seed of sea almond would possess no inherent viscosity problem. According to the present investigation, the cetane number of sea almond seed oil methyl ester is 63.39, and this shows the presence of high amount of monounsaturated fatty acids [30]. Methyl esters derived from animal sources has cloud point of about 17°C which is quite above 13°C obtained from palm oil sourced biodiesel while conversely feedstocks with lower concentrations of saturated fatty acids produces methyl esters with very low cloud point (< 0°C) [30]. Basically, biodiesel properties such as cetane number, kinematic viscosity, oxidative stability and cold flow properties are the specifications that are required to be satisfied and these have high relationship with the biodiesel fatty acid structural composition [31, 32]. Knothe [33] has reported that exhaust emission, and heat of combustion are likewise influenced by the fatty acid composition while methyl oleate is reported to be the most desired fatty acid to furnish produced biodiesel with the above expected fuel properties [1].

3.4 NMR characterization result

Nuclear magnetic resonance spectroscopy (NMR) is one of the instrumental analytical techniques used to quantify the conversion of triglycerides in vegetable oils into s [34, 35]. It is therefore, considered as one of the promising techniques for the characterization of biodiesel. The percentage conversion of the parent oil into its biodiesel using integration values for methoxy and α - carbonyl methylene protons [35] was found to be 95.7%%. Experimentally, the maximum sea almond yield obtained numerically as presented in **Table 2** and by GC maximum determination after 1 hr. were 94.21% and 93.01% respectively. All results are quite in good agreement and validate each other. The slight variation in conversion could be due to incomplete separation of FAME s from glycerine (by-product) and minor system errors as in the case of experimental and GC determinations respectively. The ^{1}H NMR spectrum of biodiesel from sea almond seed oil biodiesel is shown in **Figure 3a**. The specific peaks appearing at 0.452 ppm and 0.811 ppm for terminal methyl protons (C-CH_3) appears as singlet. From the ^{1}H NMR, the peak around 0.452 are from the terminal alkyl methyl in the s [36]. **Figure 3b** shows the ^{13}C NMR spectrum of biodiesel from the sea almond seed oil. The ^{13}C NMR shows significant aliphatic composition (CH_3) at the 24–28 ppm resonance [37] and for terminal carbon methylene at 17.774 pp. The peak at 124.629 ppm is typical of polycyclic aromatics structures [38]. Also, the peak at 167.288 ppm shows the presence of carbonyl carbon (-COO-) and O-aromatics (C-O) [34]. The peaks at 17.774–28.907 ppm could be attributed to terminal methyl groups. The unsaturation characteristics of s was confirmed by peaks appearing at δ124.629 ppm [34].

3.5 RSM optimization of sea almond seed oil methanolysis process

A central composite design (CCD) was applied to develop a correlation between the factors affecting transesterification reaction and the yield. The complete design

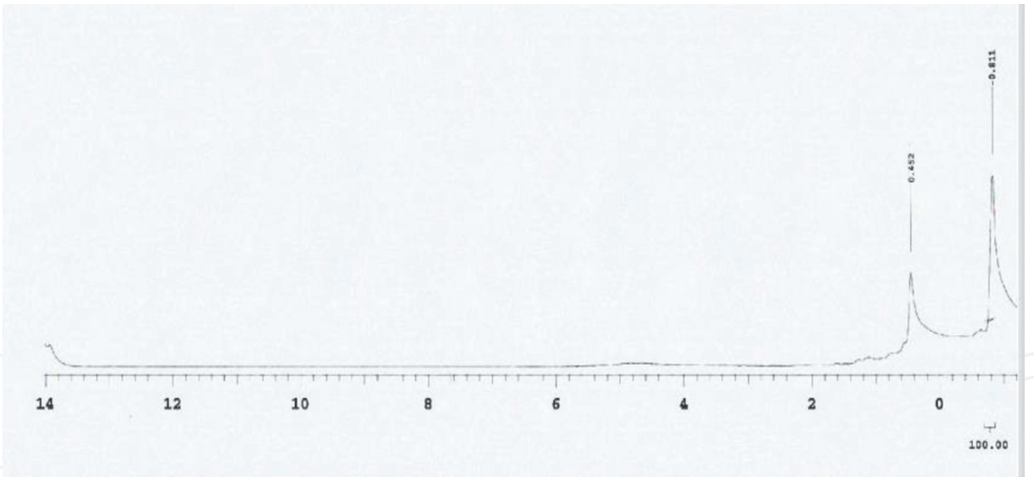

(a)

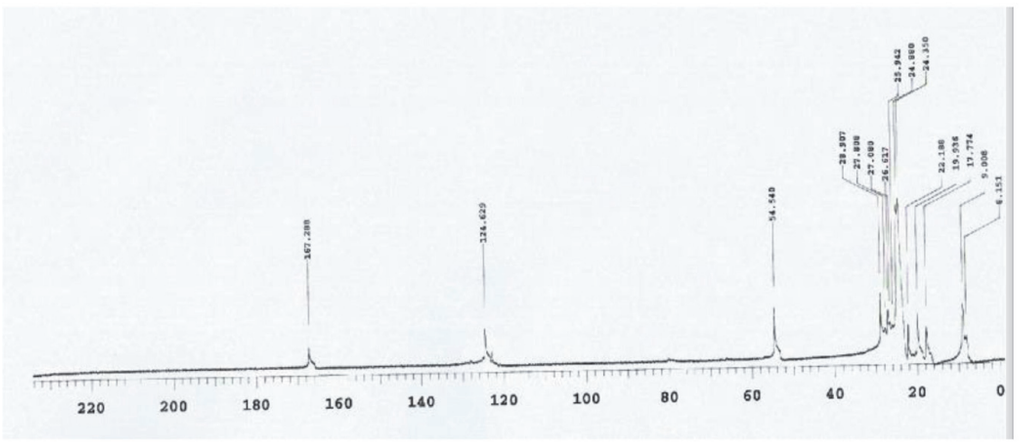

(b)

Figure 3.
(a) ^{1}H NMR spectrum of the biodiesel. (b) ^{13}C NMR spectrum of the biodiesel.

matrix, experimental and predicted responses is presented in **Table 5**. The experimental values of the content obtained were found to be in the range of ranged from 60 > actual value >95 wt %.

3.5.1 The RSM quadratic model ANOVA

The analysis of variance (ANOVA) of the RSM models (Linear, interactive linear, quadratic and cubic) were performed by considering the significance of the Fischer's F-value, lack of fit, degree of freedom (df) and R-squared (R^2). The result showed that the quadratic model best-satisfied the above set criteria. Other relevant appraisal methods involved the determination of coefficient of determination (R^2), adjusted coefficient of determination as well as coefficient of variation (C.V). These were applied to ascertain the adequacy of the model [13]. **Table 6** contains the effect of parameters using the second-order polynomial model. The following parameters X_1, X_2, X_3, $X_1 X_2$, $X_1 X_3$, $X_2 X_4$, X_1^2 and X_2^2 are found to be significant (**Table 7**). Since the parameters whose square are significant have more effect on the sea almond seed oil methanolysis [39], it implies that temperature, reaction time and catalyst had much effect on the studied response. The Model Fischer's F-value of 5.75 implies the model is significant and implies that there is only a 0.09% chance that a "Model Fischer's F-Value" this large could occur due to disturbance. The "Lack of Fit Fischer's F-value" of 0.2429 implies the Lack of Fit is not significant relative to the pure error. There is a 24.29% chance that a "Lack of Fit F-value" this

Run	Factor 1 X_1 (°C)	Factor 2 X_2 (wt %)	Factor 3 X_3 (min.)	Factor 4 X_4	Experimental value (%)	Predicted value (%)	Residual
1	40	1.0000	50	1:4000	79.8700	79.2754	0.5946
2	60	1.0000	50	1:4000	69.6400	71.6404	2.0014
3	40	2.0000	50	1:4000	65.9400	66.3137	−0.3737
4	60	2.0000	50	1:4000	68.7100	69.5587	−0.8487
5	40	1.0000	60	1:4000	83.9860	86.3597	−2.3737
6	60	1.0000	60	1:4000	86.7560	87.6047	−0.8487
7	40	2.0000	60	1:4000	83.0560	83.2380	−0.1820
8	60	2.0000	60	1:4000	85.8260	86.0330	−0.2070
9	40	1.0000	50	1:6000	66.8700	67.1823	−0.3123
10	60	1.0000	50	1:6000	70.6400	70.3273	0.3127
11	40	2.0000	50	1:6000	64.9400	65.9606	−1.0206
12	60	2.0000	50	1:6000	68.8100	69.7556	−0.9456
13	40	1.0000	60	1:6000	84.9860	84.2066	0.7794
14	60	1.0000	60	1:6000	85.7560	86.9016	−1.1456
15	40	2.0000	60	1:6000	85.0560	84.5349	0.5211
16	60	2.0000	60	1:6000	85.8260	87.3499	−1.5239
17	30	1.5000	55	1:5000	73.5780	76.3376	−2.7596
18	70	1.5000	55	1:5000	79.1180	79.3776	−0.2596
19	50	0.5000	55	1:5000	77.2780	79.7043	−2.4263
20	50	2.5000	55	1:5000	85.4180	86.0110	−0.4070
21	50	1.5000	45	1:5000	59.2320	61.6583	−2.4263
22	50	1.5000	65	1:5000	94.3640	94.1967	0.1673
23	50	1.5000	55	1:3000	76.3480	78.8357	−2.4877
24	50	1.5000	55	1:7000	76.0420	77.3425	−1.3005
25	50	1.5000	55	1:5000	75.9431	76.5521	−0.6090
26	50	1.5000	55	1:5000	75.9431	76.5527	−0.6090
27	50	1.5000	55	1:5000	75.9431	76.5521	−0.6090
28	50	1.5000	55	1:5000	75.9431	76.5521	−0.6090
29	50	1.5000	55	1:5000	75.9431	76.5521	−0.6090
30	50	1.5000	55	1:5000	75.9431	76.5521	−0.6090

Table 5.
The design matrix, experimental and predicted values of methanolysis process.

large could occur due to disturbance or noise. Non-significant lack of fit is good. It shows that the effect of most independent variables on the sea almond seed oil base methanolysis was significantly high. The non-significant lack of fit is good because it shows that the model will be well fitted [40]. The adequate precision compares the range of predicted values to the average prediction error. "Adeq Precision" measures the signal to noise ratio and a ratio greater than 4 is desirable (**Table 7**). The ratio of 8.148 obtained shows an adequate signal. The coefficient of variation is the ratio of the standard deviation of estimate to the mean value of the observed

Source	Sum of Squares	Df	Mean square	F value	p-value Prob > F	
Model	2157.2	14	154.09	5.75	0.0009	*Significant*
A- Temperature (X_1)	181.5	1	181.5	6.77	0.0200	*Significant*
B-Catalyst Conc. (X_2)	181.5	1	181.5	6.77	0.0200	*Significant*
C-Reaction Time (X_3)	190.2	1	190.2	7.09	0.0167	*Significant*
D-Metha/oil molar ratio (X_4)	28.17	1	28.17	1.05	0.3216	
AB- X_1 X_2	169	1	169	6.3	0.024	*Significant*
AC- X_1 X_3	144	1	144	5.37	0.035	*Significant*
AD- X_1 X_4	1	1	1	0.037	0.8495	
BC- X_2 X_3	36	1	36	1.34	0.2647	
BD X_2 X_4	196	1	196	7.31	0.0163	*Significant*
CD X_3 X_4	9	1	9	0.34	0.5709	
A^2 - X_1^2	1015.05	1	1015.05	37.86	< 0.0001	*Significant*
B^2 -X_2^2	304.76	1	304.76	11.37	0.0042	*Significant*
C^2 - X_3^2	92.19	1	92.19	3.44	0.0835	
D^2 - X_4^2	48.76	1	48.76	1.82	0.1975	
Residual	402.17	15	26.81			
Lack of Fit	319.33	10	31.93	1.93	0.2429	not significant
Pure Error	82.83	5	16.57			
Cor Total	2559.37	29				

Table 6.
Sea almond seed oils FAME yield response surface quadratic model ANOVA.

Std. Dev.	5.18	R^2	0.9429
Mean	76.77	Adj R^2	0.8562
C.V. %	6.75	PredR^2	0.6947
PRESS	958.64	Adeq Precision	8.148
RMSE	1.177	SEP	1.50150
MSE	1.217	AAD	0.5689

Table 7.
The regression model summary.

response and a measure of reproducibility and repeatability of the models [41]. Therefore, the C.V value of 6.75 shows the model is reasonably reproducible. Also, the R-squared of 0.9429 shows that more than 94% of the overall variability can be explained by the empirical models of the Equations. A given model significance can equally be validated when the standard deviation has a lower value than mean. Also, the smaller the PRESS-value the more the adequacy and significance of the model. Therefore, the PRESS-value obtained here supports the significance of the model. The adj. R-squared and the predicted R-squared values of 0.8562 and 0.6947 respectively for the quadratic model are in close agreement [42].

s/n	Operating variables	Sea almond[a]	Sweet almond[b]	Iranian Bitter almond[c]
1	Reaction time (min.)	58.52	65.00	60
2	Catalyst conc. (wt%)	2.04	1.5	1.4
3	Alcohol/oil molar ratio	4.66	5	9.7
4	Temperature (°C)	50.03	50	35
5	Predicted yield (wt%)	93.09	94.36	94.7
6	Experimental validated yield (wt%)	92.58	-	96.7

[a]*The present report.*
[b]*Esonye et al. [4].*
[c]*Mehdic and Kariminia [21].*

Table 8.
Optimized transesterification conditions for sea almond compared with sweet almond and Iranian bitter almond.

3.5.2 The RSM model equations

The chosen models based on coded, actual and significant terms are presented in Eqs. (18)–(20) respectively. The coded equation is useful for identifying the relative impact of the factors by comparing the factors coefficients, while the equation in terms of actual factors can be used to make predictions about the response for actual levels of each factor [40]. Analyzing the obtained model, it is observed that increase in the levels $X_1 X_2$, $X_1 X_3$, $X_1 X_4$ and $X_2 X_4$ results in a decrease in sea almond seed oil biodiesel yield [13].

$$\begin{aligned}\text{SASO FAME yield (\%w/w)} = {} & +86.83 + 2.75 * A + 2.75 * B + 0.75 * C + 1.08 * D \\ & - 3.25 * A * B - 3.00 * A * C - 0.25 * A * D \\ & + 1.50 * B * C - 3.50 * B * D + 0.75 * C * D \\ & - 6.08 * A^2 - 3.33 * B^2 - 1.83 * C^2 - 1.33 * D^2\end{aligned} \tag{18}$$

$$\begin{aligned}\text{SASO FAME yield (\%w/w)} = {} & -85.75000 + 2.75833 * \text{Temperature} \\ & + 21.37500 * \text{Cat Conc} + 2.42917 * \text{Reactionn Time} \\ & + 4.75000 * \text{Molar ratio} \\ & - 0.16250 * \text{Temperature} * \text{Cat Conc} \\ & - 0.015000 * \text{Temperature} * \text{Rxn Time} - 6.25000\text{E} \\ & - 003 * \text{Temperature} * \text{Molar ratio} \\ & + 0.15000 * \text{Cat Conc} * \text{Rxn Time} \\ & - 1.75000 * \text{Cat Conc} * \text{Molar ratio} \\ & + 0.037500 * \text{Rxn Time} * \text{Molar ratio} \\ & - 0.015208 * \text{Temperature}^2 - 3.33333 * \text{Cat Conc}^2 \\ & - 0.018333 * \text{Rxn Time}^2 - 0.33333 * \text{Molar ratio}^2\end{aligned} \tag{19}$$

$$\begin{aligned}\text{SASO FAME yield (\%w/w)} = {} & -85.75000 + 2.75833 * \text{Temperature} \\ & + 21.37500 * \text{Cat Conc} + 2.42917 * \text{Rxn Time} \\ & - 0.16250 * \text{Temperature} * \text{Cat Conc} \\ & - 0.015000 * \text{Temperature} * \text{Rxn Time} \\ & + 0.15000 * \text{Cat Conc} * \text{Rxn Time} \\ & - 1.75000 * \text{Cat Conc} * \text{Molar ratio} \\ & + 0.037500 * \text{Rxn Time} * \text{Molar ratio} \\ & - 0.015208 * \text{Temperature}^2 – 3.33333 * \text{Cat Conc}^2\end{aligned} \tag{20}$$

3.5.3 The production factors interactive effects

Figure 4A shows the 3D plot of interactive effects of reaction time and catalyst concentrations on sea almond biodiesel yield while keeping both the reaction temperature and methanol/oil molar ratio at constant zero (0) coded levels. The smoother curve of catalyst concentration axis on the 3D plots and its lesser quadratic coefficient p-values result clearly portrays that its quadratic is more significant than that of reaction time. It means that reaction time has less impact on the response than the catalyst amount. Optimum sea almond seed oil biodiesel yield was obtained at about of 58 minutes and 2.0 wt% catalyst amount and beyond these points the yield retarded. Similar range of reaction condition has been reported where highest yield of neem seed oil biodiesel was obtained at 60 min at all catalyst

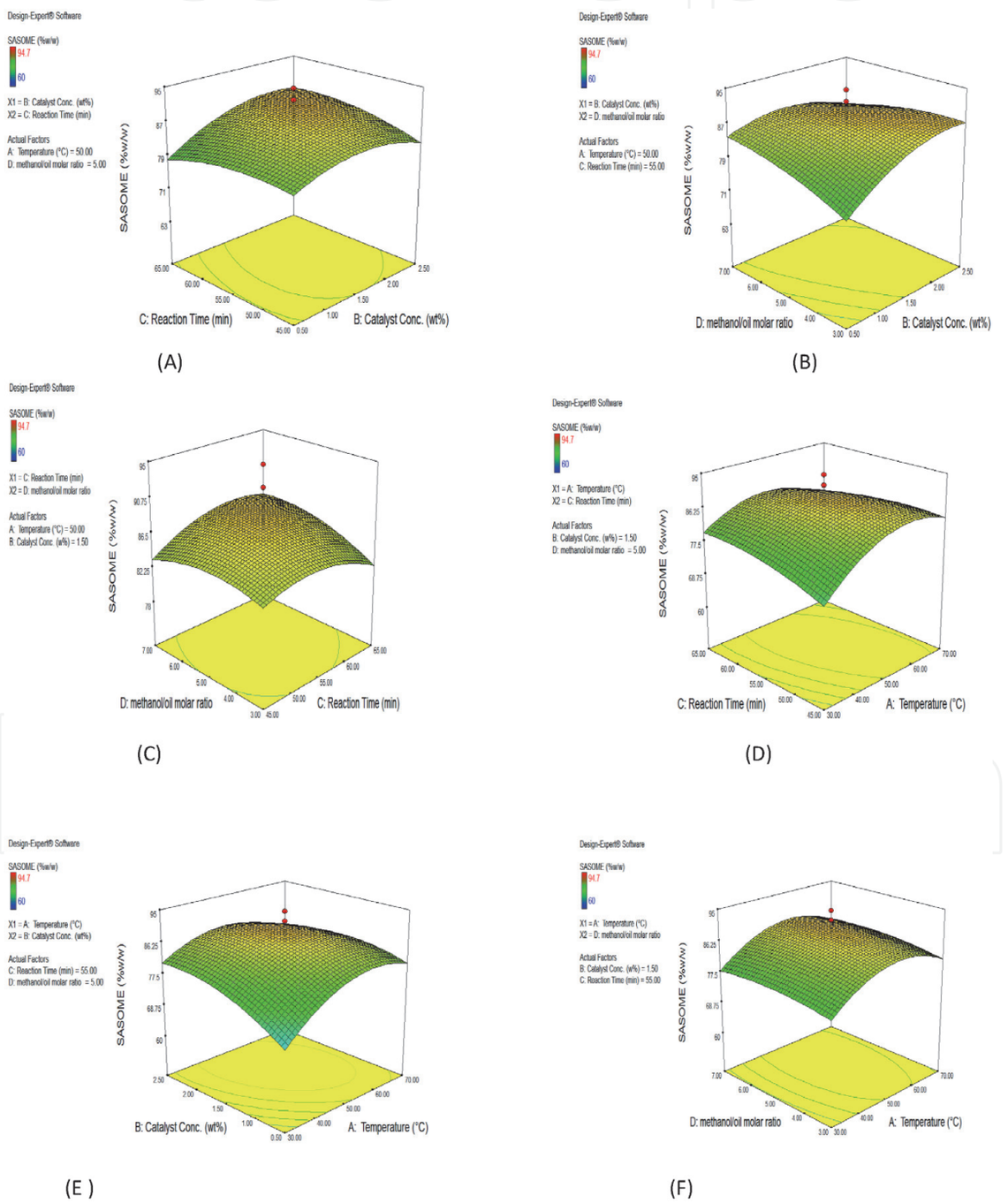

Figure 4.
The 3D response surface plot of the effects of the variables on sea almond FAME yield. (A). Reaction time and catalyst concentration. (B). Oil/methanol ratio and catalyst concentration. (C). Oil/methanol ratio and reaction time. (D). Reaction time and temperature. (E). Catalyst concentration and temperature. (F). Oil/methanol ratio and temperature.

concentration [39]. The reason could be because longer reaction time and excess catalyst promotes saponification reaction and increases in biodiesel viscosity respectively (Ofoefule, 2019). The impact of oil/methanol ratio and catalyst concentration while keeping other factors constant at 50°C and 55 minutes is represented in **Figure 4B**. The impact of both factors appears equal on the sea almond seed oil biodiesel yield and increase in both factors results in significant increase in the response. The response was observed to increase at all alcohol/oil molar ratios. However, below 2.5 wt% catalyst concentration showed increase effect on the response. Maximum yield was obtained at the highest catalyst concentration and molar ratio. Optimum yield was not attained by this combinations and this could be due to the fact that higher factors are required for them or the other factors kept constant at zero (0) levels requires shifts from the central points. Although literature reports that above these ranges, the yield decreased significantly even with increase in catalyst concentration, this could be that the excess catalyst (NaOH) reacts with methanol to form soap or produced emulsions that made the produced biodiesel had difficulty in the separation [43]. The feedstock studied here could have some deviating attributes or properties.

It was observed from **Figure 4C** that simultaneous increase in both oil/methanol molar ratio and reaction time resulted in yield increase until a certain point (6,1 and 60 min.) when it began to decrease. The smooth curves of both variables indicate that they had very significant effect on the yield of sea almond seed oil biodiesel. Both factors have almost the same impact on the biodiesel yield. Beyond these maximum points, increase in reaction time could have favored the backward reaction due to reduced concentration of the sea almond seed triglyceride while increase in molar ratio could have resulted in poor separation and recovery of glycerol [43]. This is because higher methanol content has been reported to promote high dissolution of the transesterification by-product which accelerates the reversible reaction [44]. From **Figure 4D**, the effect of reaction time and temperature while keeping other factors constant at 5.0 and 1.5 wt% for methanol/oil molar ratio and catalyst concentration respectively is presented. It shows that temperature has higher impact on the FAME yield than reaction time. The ANOVA results still show that the interactive term of temperature and reaction time was very significant while both the linear and quadratic terms of temperature were all more significant than those of reaction time similar to reports of Ofoefule et al. [13]. Basically, the higher

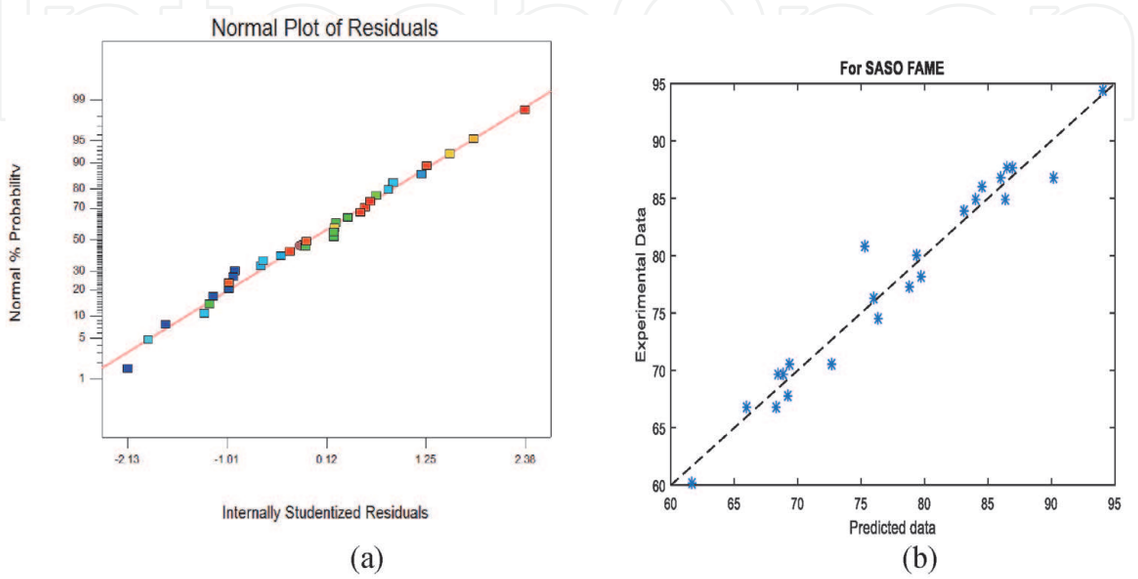

Figure 5.
(a) Normal probability plots of residuals and (b) linear correlation experimental and predicted values from sea almond seed oil methanolysis.

the temperature, the higher the reaction rate due to increase in the average kinetic energy of the reacting molecules according to Arrhenius theory [44]. The optimum temperature (60°C) would entail low cost of production as energy requirement for the seed oil methanolysis is comparatively low. Likewise, beyond 60 minutes reaction time, saponification might have been favored more due to less concentration of the reactants to push the reaction in the forward direction.

Figure 4E shows the 3D surface plot of the effects of catalyst concentration and temperature on the biodiesel yield of sea almond seed oil while keeping the reaction time and methanol/oil molar ratio constant. It shows the same trend with what was reported by Ofoefule et al. [13] on African pear seed oil biodiesel production optimization, although the catalyst concentration for the optimum yield in this report is 0.5 wt% less than what the previous report had presented. However, the explanation for the observed trend is due to increase in viscosity of the reaction composition at high catalyst concentration [13, 45]. **Figure 4F** shows the effects of oil/methanol molar ratio and temperature on the FAME yield. The catalyst concentration and reaction time was kept constant at 1.5 wt% and 55 minutes respectively. Temperature is found to have more significant impact on the response variable than methanol/oil molar ratio (as supported by the ANOVA result in **Table 6**). The FAME yield increased with increase in temperature irrespective of the value of the methanol/oil molar ratio. A reverse observation is possible if ethanol and different factor ranges were applied [43]. Optimum temperature was observed to be between 50 and 70°C in line with previous works [46].

The response values obtained by inserting the independent values are the predicted values of the model. These values are compared to the actual and experimental values. **Figure 5a** shows the normal probability plots of the residuals for clear investigations and diagnostic analysis. As it can be seen in **Figure 5b**, the data points were closely distributed along the diagonal axis. This implies that there is a good correlation between the actual and predicted values. This further corroborates the correlation between the R^2 and adjusted R^2 values. By implication, the CCD is well fitted into the model and has the capability of carrying out the optimization exercise for methanolysis of the seed oil.

The result of the optimized conditions for the optimum response of sea almond seed oil is presented in **Table 8** in comparison with the results previously reported by [4] and Mehdic and Kariminia [21] on sweet almond and Iranian bitter almond respectively. This was carried out using numerical optimization tool function of the Design Expert 7.0.0 version. The flexibility of the software enabled the generation of a total of 11 solutions together with their respective desirability. The selected best solution based on the best declared desirability of 1.00 represents the optimized process conditions where the sea almond seed oil FAME maximum response was obtained as 93.09 wt%. The chosen conditions were equally considered based on the economic point of view by taking into cognizance the impart of temperature on energy requirement, amount of catalyst and alcohol/oil molar ratio on the raw material cost and reaction time on the overall production cost. To confirm the model's adequacy, a replicate experiment was performed using the optimum points derived from the process variables and a validated yield of 92.58 wt% was obtained. The obtained result presents a good correlation between the predicted and actual biodiesel yield at the optimum levels. It is pertinent to compare optimized conditions with previous works in the literature. Here, the optimized *modus operandi* from *T. catappa* (sea almond) is compared with other reported biodiesel production processes on similar almond varieties: sweet almond and Iranian bitter almond. The conditions quite compared in yield, reaction time, and fairly on catalyst concentration. However, Iranian bitter almond biodiesel temperature of 35°C is found to be quite low compared with 50°C recorded for the other varieties. This could be due to the fact that its alcohol/oil molar ratio was about twice the values recorded for

sweet almond and sea almond varieties and the catalyst applied for Iranian bitter was KOH against NaOH applied for the other varieties. Although, sweet almond had the highest reaction time, 7°C above sea almond and 5°C above Iranian bitter almond, sea almond from this study has about 0.5 wt% catalyst higher. Above all, the three almond varieties irrespective of their climatic origin and chemical composition have similar optimum conditions for the base methanolysis of their seed oils (**Table 9**).

3.6 Chemical kinetic study results

Figure 6ai-aiii shows the variation of the intermediates of the sea almond methanolysis with time. The result obtained by observing the trend is similar to that previously reported by the authors [1]. However, there is a difference between the maximum points of last intermediates. From this work, the values were 4.8 wt% at 1.0 min and 4.98 wt% at 2.0 min at 55°C, 4.65 wt% at 1.0 min and 4.82 wt % at 2.0 min at 60°C and 4.51 wt% at 1.0 min and 4.70 at 2.0 min at 65°C. The maximum points of the last intermediates (DG) previously reported on African pear seer oil were 4.59, 4.20 and 4.10 wt% at 55°C, 60°C and 65°C respectively [1]. This difference could be due to the difference in the parent oil chemical properties. However, the results compare in values. Also, **Figure 6b** shows that the effect of temperature on the FAME yield clearly follows an increasing trend. It was observed that the difference in the concentration of FAME, within the studied temperature ranges was not significant at respective reaction times. It implies that other factors other than temperature such as reaction time, mixing intensity, etc. had more effects on the seed oil TG conversion to s. This agrees with the result of the optimization where the ANOVA showed that reaction time was more significant than temperature.

3.6.1 Second order irreversible base transesterification model

Least-square approximation was applied, in fitting a straight line to the experimental data according to a model developed based on TG hydrolysis and the second-order reaction rate as shown in Eq. (21) ([8, 18]). In each case the coefficient of determination (R^2) was determined.

Glyceride	Temperature (T)		k (wt%/min)	E_a (Kcal/mol.)
	(°C)	1/T x10^3(K^{-1})		
TG→DG	55	3.05	0.00960 (R^2 = 0.98)	12.76
	60	3.00	0.01010 (R^2 = 0.99)	
	65	2.96	0.01610 (R^2 = 0.98)	
DG→MG	55	3.05	0.00838 (R^2 = 0.98)	15.83
	60	3.00	0.00845 (R^2 = 0.97)	
	65	2.96	0.01592 (R^2 = 0.97)	
MG→Gl	55	3.05	0.01650 (R^2 = 0.98)	22.43
	60	3.00	0.02930 (R^2 = 0.99)	
	65	2.96	0.04090 (R^2 = 0.98)	

Table 9.
Summary of the kinetics result for sea almond seed oil second-order irreversible methanolysis.

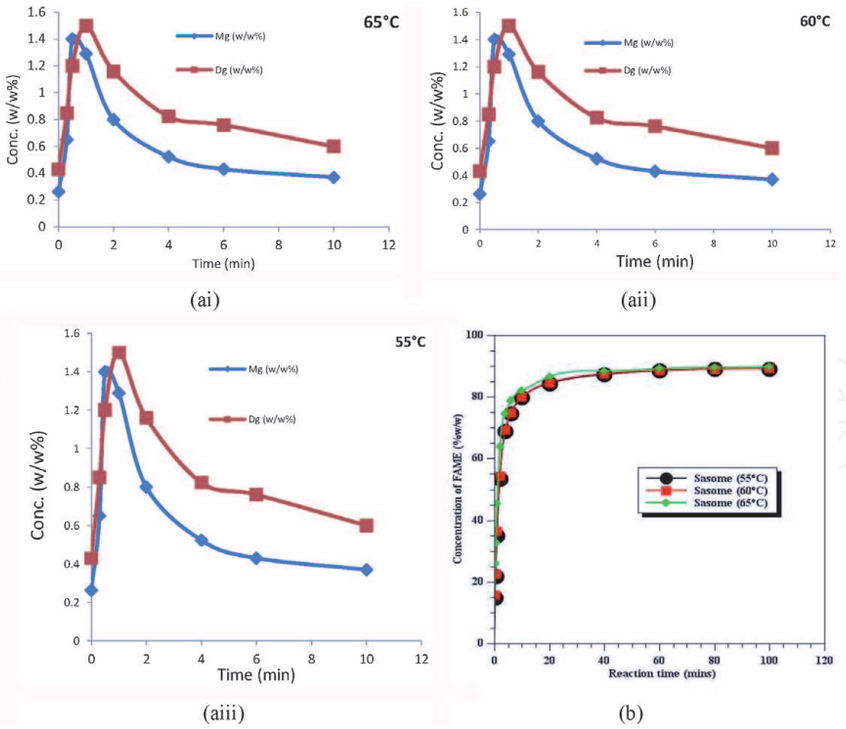

Figure 6.
(a) Progress of intermediates at various temperatures at the initial stage. (b) Effect of reaction temperature on the seed oil methanolysis.

$$\frac{-d[TG]}{dt} = k[TG]^2 \tag{21}$$

Integration of Eq. (21) gives Eq. (22).

$$k_{Tg}t = \frac{1}{[TG]} - \frac{1}{[TG0]} \tag{22}$$

Where k is the overall pseudo-rate constant, t is the reaction time, TG_0 is the initial triglyceride concentration.

A plot of reaction time (t) against $\frac{1}{[TG]}$ gave a straight line as shown in **Figure 7** with high values of coefficient (R^2) (**Table 9**) to show that the model is valid. The plot for the three temperatures (55, 60 and 65°C) is shown in **Figure 7a**, the slope is k_{TG} ($wt\%^{-1}min$). It is observed that k fairly increased with temperature. Finally, activation energies of the reaction taking place were estimated using the calculated rate constants and temperatures at which they were observed in Arrhenius equation (Eq. (17)).

The DG and MG relationship with time followed the same trend (**Figure 7b** and **c**) with that of TG. There appears to be a very close similarity in the values of activation energy obtained in this study to the previous works [8] more especially in the Triglyceride and Diglycerides hydrolysis. However, the rate constants were found to be four (4) times higher and two (2) times lower than those reported by Darnoko and Cheryan [8] on palm oil base methanolysis and Reyero et al. [6] on sun flower base-ethanolysis. The choice of feedstocks, alcohol and other factors like temperature could have resulted in the slight differences. Also, the ratio constants increase with temperature follows a trend of $k_{TG} < k_{DG} < k_{MG}$ in values. After 60 mins reaction time, the highest conversion was above 90% and it is found to be in the same range with what many other researchers have reported [1]. The hydrolysis of TG to DG is observed to be the rate determining step since it is the slowest (with smallest k) while the DG conversion to glycerol is most favored by high temperature. It is observed that

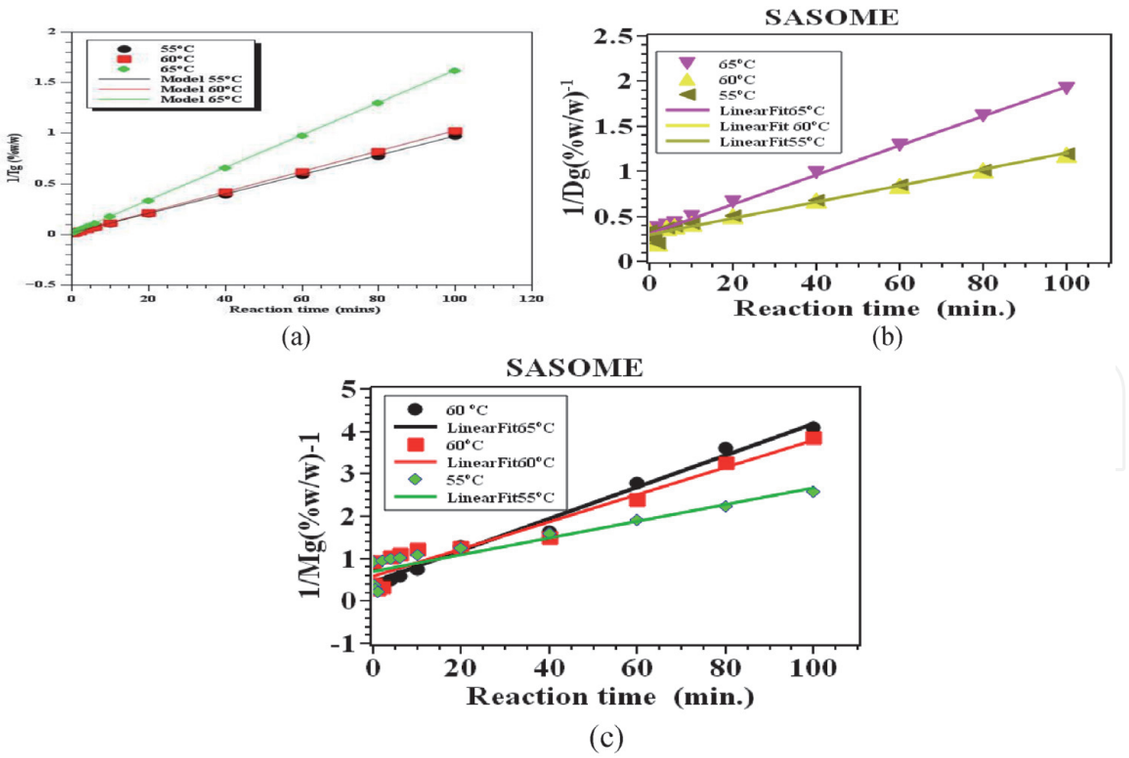

Figure 7.
Second-order reaction irreversible model of (a) triglycerides, (b) diglycerides and (c) monoglycerides hydrolysis.

Glyceride	Temperature (°C)	Reaction rate constant (min^{-1})	R^2
Triglyceride	55	0.0429	0.81
	60	0.0476	0.80
	65	0.0458	0.77

Table 10.
Summary of the rate constants for the first-order irreversible methanolysis.

all the steps have positive activation energy and this supports the endothermic characteristics of conventional transesterification process (**Figure 8**) [1].

3.6.2 First-order irreversible model

By ignoring the intermediate reactions of diglyceride and monoglyceride, the three steps have been combined in a single step [47]. However, due to the high molar ratio of methanol to oil, the change in methanol concentration can be considered as constant during reaction. This means that by taking methanol in excess, its concentration does not change the reaction order and it behaves as a first order chemical reaction [19]. The overall pseudo rate constants obtained from the slopes of the straight line plots of ln [TG] against t as shown in **Figure 9** are contained in **Table 10** for sea almond biodiesel. As can be seen from **Figure 9**, in the reactions conducted at 55, 60 and 65°C, there was a decrease in the coefficient of determination for the pseudo first-order kinetic model. **Figure 10** shows that the reaction at these temperatures does not fit the pseudo first-order reaction kinetic model better. This is supported by the lower values of coefficient of determination obtained from the first-order fitted plots ($R^2 < 0.80$) against high coefficient of determination obtained on the second-order irreversible kinetic model ($R^2 > 0.97$). Similar results have been reported on the kinetics of hydrolysis of *Nigella sativa* (*black cumin*) seed

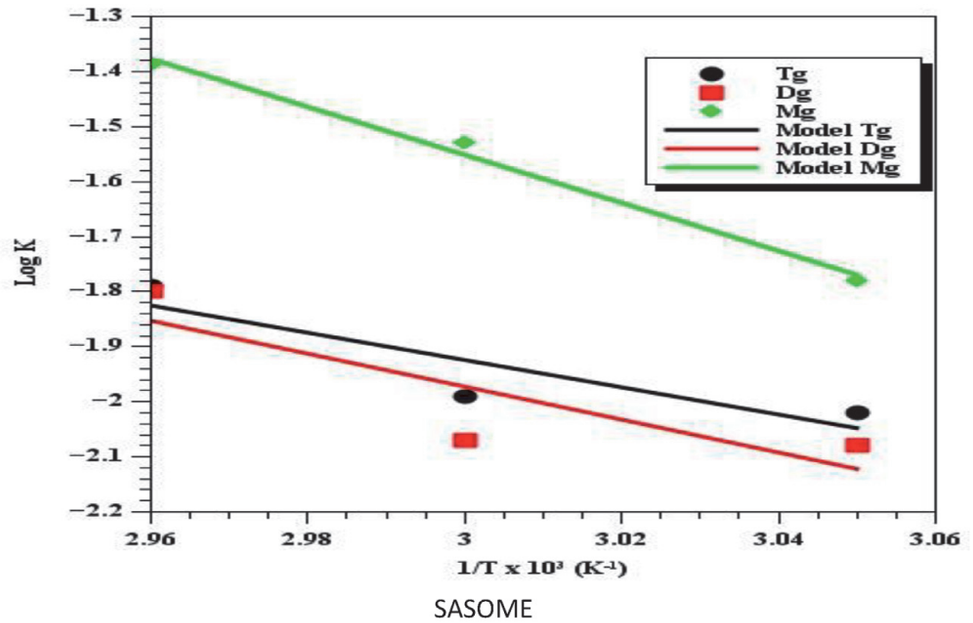

Figure 8.
Arrhenius plot of irreversible second order model reaction rate versus temperature.

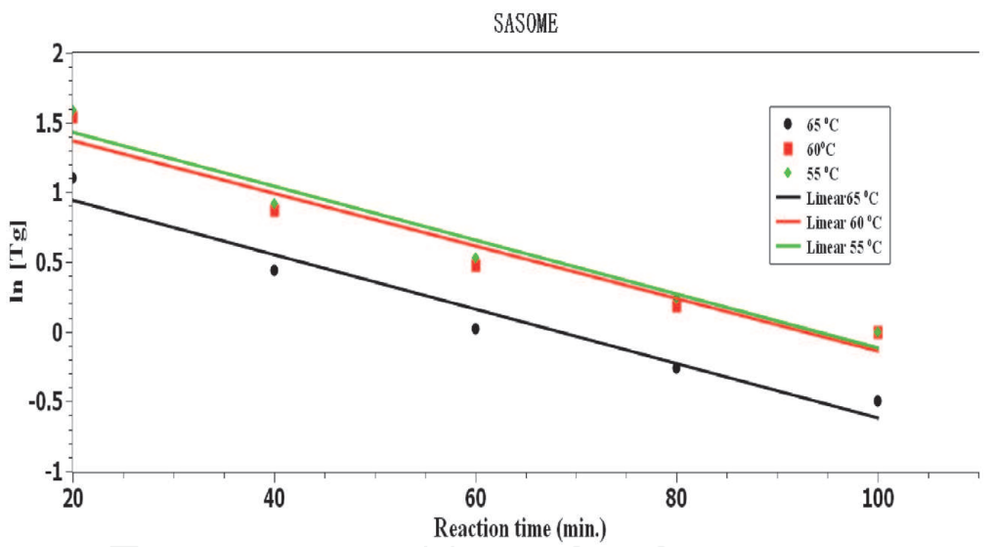

Figure 9.
First-order plot of the latter stage (from 20 minutes) triglycerides hydrolysis.

oil catalyzed by native lipase in ground seed where pseudo first-order rate equation at 20, 30 and 40°C; and the pseudo second-order equation at 50, 60 and 70°C [48]. Therefore, it could be that hydrolysis of some oils to s follows first-order irreversible kinetic models at low temperature ranges (20–40°C). The low temperature ranges is reported to favor the activity of native lipase better than at higher temperatures and this resulted in different mechanisms. But such low temperatures would not favor maximum ester yield in this study because they are far below the reported optimum temperature (Darnako and Cheryan, 2000). Darnako and Cheryan, 2000, has observed that at latter reaction stages (beyond 30 mins) of palm oil hydrolysis to, the first-order or zero-order reaction model is the best fitted. Similar observation was made on this study whereas from 20 minutes reaction, the reaction follows first-order model with high coefficient of determination ($R^2 > 0.94$). This is shown in **Figure 10**. These stages showed low reaction rate due to reduction in the reactants concentration. It implies that at low temperatures and latter stages of methanolysis of the vegeatble oils progesses very slowly and follow first-order kinetic model.

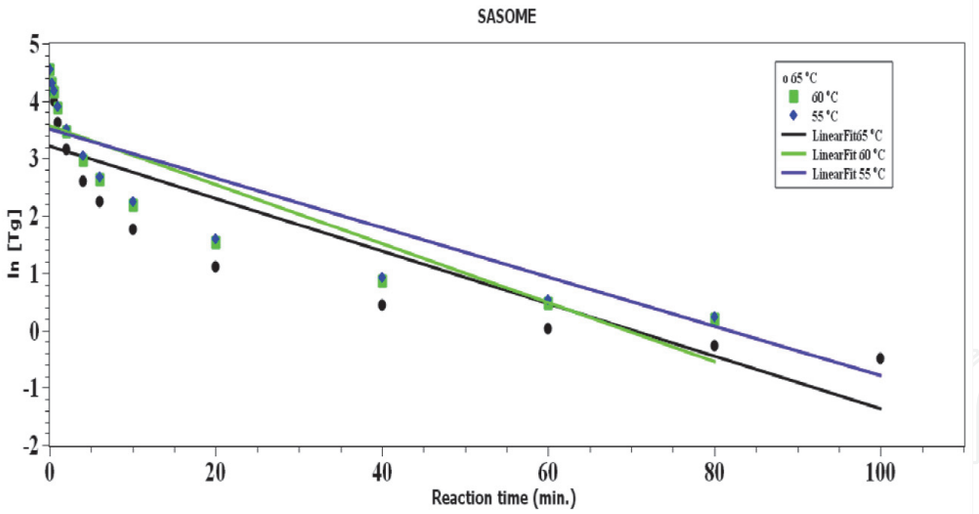

Figure 10.
First-order plot of the triglycerides hydrolysis.

4. Conclusion

The statistical optimization and chemical reaction kinetics of consecutive irreversible second order alkali- transesterification of *terminalia cattapa* seed oil has been successfully achieved and reported. RSM from Design Expert 7.0.0 version software was used for optimizing and predicting the process conditions in line with standard methodologies. The optimum conditions of base methanolysis process of the sea almond seed oil was obtained at favorable economic standpoint considering cheap materials requirement, low energy consumption and fast production rate. At low temperatures and latter stages, the methanolysis progresses very slowly and followed first order kinetic model but the irreversible second-order model of the power rate law best described the conversion of triglycerides with time at all stages. The data generated from the statistical optimization and chemical kinetics evaluations are found to be complimentary. The ‘s unsaturated characteristics would enhance its cold flow properties. The fuel properties of the biodiesel produced compared well with international standards. This research would help in commercial production of biodiesel from *T. cattapa* on industrial scale.

Acknowledgements

The authors would like to thank the staff and management of the PZ/NOTAP Chemical Engineering laboratory of Alex Ekwueme Federal University, Abakaliki, Nigeria for the availability of the laboratory facilities, apparatus and analytical equipment.

Conflict of interest

The authors hereby declare no competing financial interest.

Funding

This research did not receive any specific grant from any funding agent in public, commercial or not-for-profit-sectors.

Data availability

Research data are not shared

Notations

[Al]	Alcohol concentration
Al	Alcohol
DG	Diglycerides
[DG]	Diglycerides concentration
E_a	Activation energy (kcal/min)
FAAE	Fatty acid alkyl ester
FAEE	Fatty acid ethyl ester
FAME	Fatty acid methyl ester
Gl	Glycerol
[Gl]	Glycerol concentration
k_1-k_3	Rate constants (wt%/.min)
k_0	Frequency factor
MG	Monoglycerides
[MG]	Monoglycerides concentration
SASO	sea almond seed oil
SASOME	sea almond seed oil methyl ester
T	Temperature (K or °C)
TG	Triglyceride
[TG]	Triglyceride concentration

Author details

Chizoo Esonye[1*], Okechukwu Donminic Onukwuli[2], Akuzuo Uwaoma Ofoefule[3], Cyril Sunday Ume[1] and Nkiruka Jacintha Ogbodo[1]

1 Department of Chemical Engineering, Alex Ekwueme Federal University, Ndufu-Alike, Abakaliki, Nigeria

2 Department of Chemical Engineering, Nnamdi Azikiwe University, Awka, Nigeria

3 Department of Industrial and Applied Chemistry, University of Nigeria, Nsukka, Nigeria

*Address all correspondence to: eso_vic@yahoo.com; esonye.chizoo@funai.edu.ng

References

[1] Esonye C, Onukwuli OD, Ofoefule AU. Chemical kinetics of a two-step Transesterification of Dyacrodes Edulis seed oil using acid-alkali catalyst. Chemical Engineering Research and Design. 2019a;**145**:245-257 http://dx.doi.org/10.1016/j.cherd.2019.03.010

[2] Patil P, Gude VG, Pinappu S, Deng PS. Transesterification kinetics of Camelina sativa oil on metal oxide cata; lysts under conventional and microwave heating condions. Chemical Engineering Journal. 2011;**168**:1296-1300

[3] Chatterjee S, Kumar A, Basu S, Dutta S. Application of response surface methodology for methylene blue dye removal from aqueous solution using low-cost adsorbent. Chemical Engineering Journal. 2012;**181-182**: 289-299

[4] Esonye C, Onukwuli OD, Ofoefule AU. Optimization of production from Prunus Amygdalus seed oil using response surface methodology and artificial neural networks. Renewable Energy. 2019b;**130**(62–71) http://dx.doi.org/10.1016/j.renene.2018.06.036

[5] Sarve A, Varma MN, Sonawane SS. Response surface optimization and artificial neural network modeling of biodiesel production from crude mahua (Mahua indica) oil under supercritical ethanol condition using CO_2 as co-solvent. Royal Society of Chemists Advances. 2015;**5**:69702-69713

[6] Reyero JG, Arzamendi S, Zabala ML, Gandia P. Kinetics of NaOH-catalyzed transesterification of sun flower oil with ethanol to produce biodiesel. Fuel Processing Technology. 2015;**129**: 147-155

[7] Jansri SS, Ratanawilu B, Allen ML, Prateepchaukul G. Kinetics of production from mixed crude oil by using acid-alkali catalyst. Fuel Processing Technology. 2011;**92**: 1543-1548

[8] Darnoko D, Cheryan M. Kinetics of palm oil transesterification in a batch reactor. Journal of the American Oil Chemists' Society. 2000;**77**:1263-1267

[9] Ilgen O. Reaction kinetics of dolomite catalyzed transesterification of conola oil and methanol. Fuel Processing Technology. 2012;**95**:62-66

[10] Weerawatanakorn M. Terminalia catappa seeds oil as a new dietary healthy oil source. In: The Annual Meeting of the International Society for Nutraceuticals and Functional Foods (ISNFF). Taipei, Taiwan; 2013

[11] Menkiti MC, Agu CM, Udeigwe TK. Kinetic and parametric studies for the extractive synthesis of oil from *Terminalia catappa* L. kernel. Reac Kinet Mech Cat. 2016. DOI: 10.1007/s11144-016-1101-y

[12] Monnet, Y. T, Gbogeuri A, Kouadio P, Koffi B, & Kouame, L. P. (2012) Chemical characterization of seeds and seed oil from mature Terminalia catappa fruits harvested in cote d'Ivoire. Int J Biosci10:110–124.

[13] Ofoefule AU, Esonye C, Onukwuli OD, Nwaeze E, Ume CS. Modeling and optimization of African pear seed oil esterification and transesterification using artificial neural network and response surface methodology comparative analysis. Industrial Crops and Products. 2019. DOI: 10.1016/j.indcrop.2019.111707

[14] AOAC (2000).Official methods of analysis, (13^{th} edition), Association of Official Analytical Chemists, Washington, DC

[15] Furnish BS, Hannaford AJ, Smith PWG, Tatchell AR. Vogel's Textbook of

Practical Organic Chemistry. 5th ed. UK: Longman group; 1989. pp. 1412-1422

[16] Fu YJ, Zu YG, Wang LL, Zhang NJ, Liu W, Li SM, et al. Determination of fatty acid s in biodiesel produced from yellow horn oil by RP-LC-RID. Chromatographia. 2008;**67**:9-14

[17] Betiku E, Ajala SO. Modeling and optimization of Thevetia peruviana (yellow oleander) oil biodiesel synthesis via Musa paradisiacal (plantain) peels as heterogeneous base catalyst: A case of artificial neural network vs response surface methodology. Industrial Crops and Products. 2014;**53**:314-322

[18] Levenspiel O. Chemical Reaction Engineering. 3rd ed. McGraw-Hill; 1999

[19] Zhang L, Sheng B, Xin Z, Liu Q, Sun S. Kinetics of transesterification of palm oil and dimethyl carbonate for biodiesel production at the catalysis of heterogeneous base catalyst. Bioresource Technology. 2010;**101**: 8144-8150

[20] Kumar GR, Ravi R, Chadh A. Kinetic studies of base-catalyzed transesterification reaction of non edible oils to prepare biodiesel; the effect of co-solvent and temperature. Energy and Fuels. 2011;**25**:2826-2832

[21] Mehdic A, Kariminia H. Optimization of biodiesel production from Iranian bitter almond oil using statistical approach. Applied Energy. 2011;**88**(7):2377-2381

[22] Ndana M, Grace JJ, Baba FH, Mohammed UM. Fourier transform infrared spectrometyric analysis of functional groups in biodiesel produced from oil of recinum communis, hevea brasiliences and jatropha curcas seeds. Int. J. of Sc. Envi. & Tech. 2013;**2**(6): 1116-1121

[23] Saifuddin N, Refai H. Spectroscopy analysis of structural transesterification in biodiesel degradation. Research Journal of Applied Sciences, Engineering and Technology. 2014;**8**(9): 1149-1159

[24] Conceicao MM, Fermardes VJ, Araiyo AS, Farais MF, Santos IM, Souza AG. Thermal and oxidative degradation of castor oil biodiesel. Journal of Energy Fuel. 2007;**21**(1):1522-1527

[25] Gunstone ED. Rapeseed and canola oil: Production process, properties and uses. JAOCS. 2004;**33**:132-139

[26] Knothe G. Improving biodiesel fuel properties by modifying fatty ester composition. Energy and Environmental Science. 2009;**2**:759-766

[27] Sharma YC, Singh B. Development of biodiesel current scenarior. Review Sustain. Energy Rev. 2009;**13**(6–7): 1646-1651

[28] Esonye C, Onukwuli OD, Ofoefule AU, Ogah EO. Multi-input multi-output (MIMO) ANN and Nelder-Mead's simplex based modeling of engine performance and combustion emission characteristics of biodiesel-diesel blending CI diesel engine. Applied Thermal Engineering. 2019c;**151**:100-114 http://dx.doi.org/10.1016/j.applthermaleng.2019.01.101

[29] Knothe G. Determing the blend levels of mixtures of biodiesel with conventional diesel fuel by fibre-optic near infra red spectroscopy and H magnetic resonance spectroscopy. J. America Oil Chem. Sci. 2001;**78**:1025

[30] Koria L, Nithya G. Analysis of Datura stramonium Linn, biodiesel by GC –MS and influence of fatty acid composition on fuel related characteristics. Journal of Phytology. 2012;**4**(1):06-09

[31] Knothe G. Biodiesel and renewable diesel: A comparison. Progress in Energy

and Combustion Science. 2010;**36**(3): 364-373

[32] Mittlebach M, Remschnodt C. Biodiesel the Comprehensive Handbook. Vienna: Boersedruck Ges MBH; 2004

[33] Knothe G. Synthesis and characterization of long chain 1, 2-dioxo compounds. Chemistry and Physiscs of lipids. 2012;**50**:14-34

[34] Mushtaq A, Shazia S, Lee KT, Ahmed ZA, Haleema S, Muhammed Z, et al. Distaff thistle oil: A possible new non-edible feedstock for biogas energy. International Journal of Green Energy. 2014;***10***:1-27

[35] Naureen R, Tariq M, Yusoff I, Chowdhury AJK, Ashraf MA. Synthesis, spectroscopic and chromatographic studies of sunflower oil biodiesel using optimized base catalysed methanolysis. Saudi Journal of Biological Sciences. 2015;**22**:332-339

[36] Nagaraja YP, Venkatesh HS, Vinoyty MS. Production of biodiesel from poultry waste. International Journal of Pharma and Bio Sciences. 2014;**592**:791-799

[37] Novak JM, Lema T, Xing B, Gaaskin JW, Steiner C, Das KC, et al. Characterization of designer biochar produced at different temperatures and their effects on a loamy sand. Ani Environ Sc. 2009;**3**:195-206

[38] Novotry, E. H., deAzevedo E. R., Bonagamba J. J. Cunha, T. J. F, Mmadari B. E. de M. Benites, V. & Hayes M. H. B. (2007) Studies of the compositions of humic ascids from Amazoruan Dark Earth Soils. Environ. Sc. Technol 41: 400–405.

[39] Awolu OO, Layokun SK. Optimization of two-step transesterification production of biodiesel from neem (Azadirachta indica) oil. Int. J. of Energy and Environmental Engineering. 2013;**4**:39

[40] Ohale PE, Uzoh CF, Onukwuli OD. Optimal factor evaluation for the dissolution of alumina from azaraegbelu clay in acidic solution using RSM and ANN comparative analysis. South African Journal of Chemical Engineering. 2017;**21**:43-54

[41] Chen, G., Chen, J., Srinivasakannan, C., & Peng., J. (2011). Application of response surface methodology for optimisation of the synthetic nitrile from titania slag. App. Surf. Sci. 268 (7) 3068–3073,

[42] Uzoh CF, Onukwuli OD, Ozofor IH, Odera RS. Encapsulation of urea with alkyd resin-starch membranes for controlled N_2 release: Synthesis, characterization, morphology and optimum N_2 release. Process Safety and Environmental Protection. 2019;**121**: 133-142

[43] Silva GF, Fernando L, Camargo F, Andrea LO, Ferreira F. Application of response surface methodology for optimization of biodiesel production by transesterification of soybean oil with ethanol. Fuel Processing Technology. 2011;**92**:407-413

[44] Ayodele A, Ayoola KF, Hymore KF, Omonhinmin CA. Optimization of biodiesel production from selected waste oils using response surface methodology. Biotechnology. **2017**;**16**:1-9

[45] Tshizanga N, Aransiola EF, Oyekola O. Optimisation of biodiesel production from waste vegetable oil and eggshell ash. South African Journal of Chemical Engineering. 2017;**23**:145-156

[46] Odude VO, Adesina AJ, Oyetunde OO, Adeyemi OO, Ishola NB, Anietie Okon Etim AO, et al. Application of agricultural waste-based catalysts to Transesterification of esterified palm

kernel oil into biodiesel: A case of Banana fruit Peel versus cocoa pod husk. Waste and Biomass Valorization. 2017 https://doi.org/10.1007/s12649-017-0152-2

[47] Birla A, Singh B, Upadhyay S, Sharma Y. Kinetics studies of synthesis of biodiesel from waste frying oil using a heterogeneous catalyst derived from snail shell. Bioresource Technology. 2012;**106**:95-100

[48] Dandik L, Aksoy HA. The kinetics of hydrolysis of Nigella sativa (black cumin) seed oil catalyzed by native lipase in ground seed. JAOCS. 1992;**69** (12):1239-1240